# Proline-Directed Phosphorylation of the Dopamine Transporter N-Terminal Domain[†]

Balachandra K. Gorentla, Amy E. Moritz, James D. Foster, and Roxanne A. Vaughan*

*Department of Biochemistry and Molecular Biology, School of Medicine and Health Sciences, University of North Dakota, Grand Forks, North Dakota 58201*

*Received September 5, 2008; Revised Manuscript Received December 24, 2008*

ABSTRACT: Phosphorylation of the dopamine transporter (DAT) on N-terminal serines and unidentified threonines occurs concomitantly with protein kinase C (PKC)- and substrate-induced alterations in transporter activity, subcellular distribution, and dopamine efflux, but the residues phosphorylated and identities of protein kinases and phosphatases involved are not known. As one approach to investigating these issues, we recombinantly expressed the N-terminal tail of rat DAT (NDAT) and examined its phosphorylation and dephosphorylation properties in vitro. We found that NDAT could be phosphorylated to significant levels by PKCα, PKA, PKG, and CaMKII, which catalyzed serine phosphorylation, and ERK1, JNK, and p38, which catalyzed threonine phosphorylation. We identified Thr53, present in a membrane proximal proline-directed kinase motif as the NDAT site phosphorylated in vitro by ERK1, JNK and p38, and confirmed by peptide mapping and mutagenesis that Thr53 is phosphorylated in vivo. Dephosphorylation studies showed that protein phosphatase 1 catalyzed near-complete in vitro dephosphorylation of PKCα-phosphorylated NDAT, similar to its in vivo and in vitro effects on native DAT. These findings demonstrate the ability of multiple enzymes to directly recognize the DAT N-terminal domain and for kinases to act at multiple distinct sites. The strong correspondence between NDAT and rDAT phosphorylation characteristics suggests the potential for the enzymes that are active on NDAT in vitro to act on DAT in vivo and indicates the usefulness of NDAT for guiding future DAT phosphorylation analyses.

The dopamine transporter (DAT)[1] is a plasma membrane phosphoprotein expressed in dopaminergic neurons that clears synaptic dopamine (DA) by $Na^+-Cl^-$-dependent reuptake. This activity controls the availability of extracellular DA for binding to receptors and, thus, regulates the dynamics of dopaminergic neurotransmission (*1*). Processes controlled by DA include motor activity, emotion, and reward, and agents such as cocaine that inhibit DAT cause elevations in DA levels that lead to motor stimulation and addiction (*2*). DA levels are also increased by amphetamine (AMPH) and methamphetamine (METH), which are carried by DAT and induce DA efflux by the process of reverse transport (*3, 4*). It is thought that dopaminergic disorders, such as depression, schizophrenia, ADHD and Parkinson's disease, may be linked to dysregulation of DAT activity and resulting imbalances in DA clearance (*5*−*9*).

Various properties of DAT are acutely regulated by protein kinases, protein phosphatases, and substrate pretreatments (*10*−*12*), indicating the ability of DAT to rapidly respond to physiological demands. Regulation of DA transport occurs in response to modulation of protein kinase C (PKC), extracellular signal-regulated protein kinase (ERK), protein kinase B (Akt), and protein phosphatases 1 and 2A (PP1/2A) (*13*−*16*), and PKC activity is required for substrate-induced transport down-regulation (*17*−*19*). Kinase- and substrate-induced DA transport down-regulation are associated with alterations in DAT trafficking and surface levels (*16, 20*−*24*), while PKC-induced transport regulation also occurs in part by a trafficking-independent process that is sensitive to cholesterol depletion (*25*). Basal and AMPH-stimulated DA efflux involve actions of PKC and CaMKII (*4, 15, 26*), and activation of PKC stimulates DAT phosphorylation, ubiquitylation and degradation (*13, 27, 28*). Thus, it is clear that several functions of DAT are regulated by multiple phosphorylation pathways. The precise mechanisms by which most of these effects occur remain unknown, although DAT N-terminal phosphorylation has been reported to be required for AMPH-induced efflux and AMPH/METH-induced increases in intracellular $Ca^{2+}$ (*29*) but not for PKC or AMPH-induced DAT endocytosis and down-regulation (*18, 30*).

In both rat striatal tissue and heterologous expression systems, DAT displays a tonic level of phosphorylation that is increased by PKC activators, such as phorbol 12-myristate 13-acetate (PMA), and phosphatase inhibitors, such as

[†] This work was supported by grants R01 DA13147 to R.A.V. from the National Institute on Drug Abuse, ND EPSCoR IIG to R.A.V. and J.D.F., ND EPSCoR Doctoral Dissertation Fellowship to B.K.G., P20 RR016741 to the University of North Dakota from the INBRE program of the National Center for Research Resources, and ND EPSCoR through NSF EPS-0447679.

* To whom correspondence should be addressed. Telephone: 701-777-3419. Fax: 701-777-2382. E-mail: rvaughan@medicine.nodak.edu.

[1] Abbreviations: DAT, dopamine transporter; DA, dopamine; AMPH, amphetamine; METH, methamphetamine; PKC, protein kinase C; PKA, cAMP dependent protein kinase; PKG, cGMP dependent protein kinase; CAMKII, calcium−calmodulin protein kinase II; ERK, extracellular signal-regulated kinase; PMA, phorbol 12-myristate, 13-acetate; OA, okadaic acid; PP1, protein phosphatase 1; PP2A, protein phosphatase 2A; PP2B, protein phosphatase 2B; pSer, phosphoserine; pThr, phosphothreonine; NDAT, N-terminal domain DAT recombinant protein; CDAT, C-terminal DAT recombinant protein.

10.1021/bi801696n CCC: $40.75 
Published on Web 01/15/2009

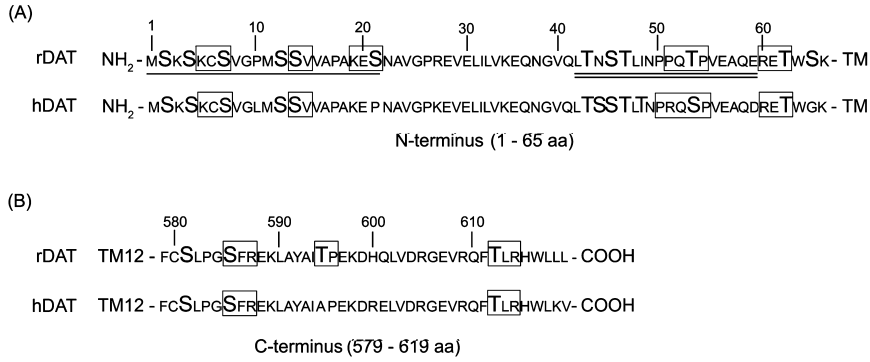


FIGURE 1: DAT N- and C-terminal domains. Amino acid sequences of rat and human DAT N-termini (A) and C-termini (B). Serines and threonines are highlighted in large font, and consensus motifs for PKC, PKA, CaMK, and proline-directed kinases are enclosed by boxes. The N-terminal serine cluster of rDAT containing known in vivo phosphorylation sites is indicated with the single underline, and the epitope for Ab16 is shown with the double underline.

okadaic acid (OA) (*13, 18, 30, 31*), implicating the activities of PKC and PP1/2A in DAT phosphate turnover. Reduced DAT phosphorylation has been found after pharmacological inhibition of ERK (*32*), suggesting a role for this kinase in maintenance of DAT phosphorylation. DAT phosphorylation is also stimulated by in vivo and in vitro AMPH and METH treatments via a PKC-dependent process (*18*), and PMA-induced phosphorylation is inhibited by in vitro application of the DA uptake blocker GBR12909 (*19*) and at low PMA concentrations by cocaine (*33*), indicating a role for psychoactive drugs in the regulation of transporter phosphorylation and the accompanying processes. In addition, serine mutagenesis studies have suggested the phosphorylation of DAT by CaMKII as a mechanism underlying AMPH-induced DA efflux (*15*).

PKC- and OA-stimulated metabolic phosphorylation of rat striatal DAT has been mapped to a cluster of six closely spaced serines at the distal end of the N-terminal tail (Figure 1A) (*34*), and mutagenesis of heterologously expressed rat (r) and human (h) DAT has confirmed utilization of sites in this domain (*18, 30*). The precise residues within this domain that are phosphorylated remain unknown, although mutation and deletion studies indicate the use of multiple sites (*32, 35*). This region contains consensus motifs for PKC, cAMP-dependent protein kinase (PKA), and CaMKII, while a second cluster of serines and threonines more proximal to the membrane contains consensus motifs for PKC, PKA, and proline-directed kinases (Figure 1A). The DAT C-terminal tail also contains canonical PKC, PKA, and proline-directed kinase motifs (Figure 1B). Although Ser and Thr residues in the C-terminal domain have been suggested as potential phosphorylation sites (*36*), little evidence currently supports this. Thus, the N- and C-termini contain multiple potential phosphorylation sites for many of the kinases that affect DAT phosphorylation and/or regulation, but it is not known if these enzymes directly phosphorylate DAT, and if so, at which sites. This information is necessary for understanding the mechanisms by which phosphorylation regulates DAT and determining if kinase-mediated regulatory processes occur through phosphorylation of DAT or through effects on interacting proteins.

As one approach to investigating these issues, we recombinantly expressed the N- and C-terminal domains of rDAT (NDAT and CDAT) and used the peptides for in vitro phosphorylation and dephosphorylation studies. Our results show that NDAT is an excellent substrate for multiple protein kinases and phosphatases, and that different kinases act on the peptide at different sites. This demonstrates the ability of these enzymes to directly interact with DAT and indicates the potential for these enzymes to act on DAT in vivo. Robust NDAT in vitro threonine phosphorylation catalyzed by proline-directed kinases was found at Thr53, and mutagenesis of Thr53 in the full-length protein caused loss of metabolically incorporated phosphothreonine, identifying this residue as the origin of phosphothreonine in DAT and providing the first evidence for proline-directed phosphorylation of DAT.

## METHODS

*Cloning of DAT N- and C-Terminal Domains.* The rDAT N- and C-terminal tail sequences shown in Figure 1 (NDAT and CDAT) were inserted into Intein recombinant expression vectors that fuse the protein of interest to Chitin Binding Domain (CBD, molecular mass ~55 kDa) via a sulfhydryl-cleavable bond. The wild-type (WT) rDAT cDNA in a pcDNA 3.0 vector (*18*) was used for cloning. The open reading frame encoding amino acids 1−65 was PCR amplified and subcloned into the pTYB2 expression vector (New England Biolabs, Ipswich, MA) to generate NDAT linked via its C-terminus to CBD. The open-reading frame encoding amino acids 579−619 was amplified and subcloned into the pTYB1 expression vector to generate CDAT linked via its N-terminus to CBD. NDAT threonine (T) to alanine (A) substitutions were generated in the pTYB2-NDAT construct using the Stratagene QuikChange kit. Accuracy of all constructs was verified by sequencing (Alpha Biolabs, CA).

*Expression and Purification of NDAT and CDAT. E. coli* T7 express cells (New England Biolabs, Ipswich, MA) were transformed with NDAT-pTYB2 or CDAT-pTYB1, and colonies were selected from LB agar plates containing 50 $\mu$g/mL of carbenicillin. Transformed colonies were inoculated into LB medium containing 50 $\mu$g/mL carbenicillin and grown at 37 °C to an $OD_{600}$ of 0.8. Fusion protein expression was induced with 0.5 mM isopropyl $\beta$-D-1-thiogalactopyranoside (IPTG) for 16 h at 16 °C. Bacteria were pelleted by centrifugation at 5000*g* for 10 min at 4 °C, resuspended with ice-cold lysis buffer (50 mM Tris, pH 7.5, 150 mM NaCl, 0.05% Triton X-100 and one Roche Complete Mini protease inhibitor tablet), and lysed by passage through a French pressure cell. The resulting crude extract was centrifuged at 20000*g* for 30 min to sediment particulate

elements, and analysis of pellets and supernatants indicated >95% recovery of NDAT−CBD and CDAT−CBD in the soluble fraction.

NDAT−CBD and CDAT−CBD fusion proteins were isolated from crude *E. coli* lysate by chromatography on chitin−Sepharose. Lysates were incubated with chitin−Sepharose resin for 18 h at 4 °C, the unbound fraction was collected, and the resin was washed with 10 bed volumes of column buffer (50 mM Tris, pH 7.5, 500 mM NaCl, 1 mM EDTA). NDAT and CDAT were released from CBD by two sequential incubations of the resin with 3 bed volumes of column buffer containing 50 mM dithiothreitol (DTT) for 40 h at 4 °C. The eluted fragments were dialyzed extensively against 20 mM MOPS pH 7.4, and concentrated to 1−10 mg/mL by spin filtration. Protein levels were determined using the BioRad protein assay kit and peptides were estimated to be >95% pure by Commassie staining.

*In Vitro Phosphorylation Assays.* NDAT or CDAT (1.5 $\mu$g) was suspended in 20 mM MOPS pH 7.4 containing 5 mM $MgCl_2$, 300 $\mu$M $CaCl_2$, 40 $\mu$M ATP, 12 $\mu$Ci [$\gamma$-$^{32}$P]ATP, and additional components as indicated below in a final volume of 75 $\mu$L. Reactions were initiated by adding purified recombinant kinases and were performed at 30 °C for 30 min and terminated by addition of 100 mM EDTA. Additional specific reagents included were 40 $\mu$g/mL dioleoylphosphatidylserine and 1.6 $\mu$g/mL diacylglycerol for all PKC isoforms, 2.4 $\mu$M calmodulin for CaMKII, and 10 $\mu$M 8-Br cGMP for PKG. Enzyme amounts used were calculated to provide equal specific activities (1 nmol of phosphate transfer to model substrate/min) based on information provided by vendors, and all kinases were highly active against histones or myelin basic protein (not shown). Following in vitro phosphorylation, NDAT and CDAT samples were immunoprecipitated with polyclonal antibody (Ab) 16 generated against rDAT N-terminal amino acids 42−59 (Figure 1A) or DAT C-terminal antibody from Chemicon. Precipitated samples were electrophoresed on 10−20% SDS polyacrylamide gels using low- and high-range Rainbow molecular mass markers as standards, and gels were dried and subjected to autoradiography at −70 °C using Kodak Biomax film for 2−48 h or were transferred to PVDF for immunoblotting. For immunoblotting, PVDF membranes were probed with DAT N-terminal monoclonal Ab16 (mAb16) and developed as described (*37*). Autoradiographs and immunoblots were scanned and band densities quantified with BioRad Molecular Analyst software (*19, 31*). For quantification of relative in vitro phosphorylation levels, the densitometric values of NDAT phosphorylated by PKC$\alpha$ or ERK1, as indicated, were normalized to 100% and values for other kinases expressed as a fraction thereof. All experiments were performed two or more times with similar results.

*In Vitro Dephosphorylation Assay.* NDATs phosphorylated in vitro by PKC$\alpha$ or ERK1 were immunoprecipitated with Ab16 and in vitro dephosphorylation was assessed in triplicate using immune complexes bound to protein A Sepharose beads. The reaction mixtures consisted of 20 mM MOPS pH 7.4, 200 $\mu$M $MnCl_2$, 5 mM DTT, 100 $\mu$M EDTA, 0.2% BSA and purified PP1, PP2A, or PP2B, in a final volume of 500 $\mu$L. PP2B reactions also contained 1 $\mu$M calmodulin and 1 mM $CaCl_2$. Enzyme amounts used were calculated to provide equal specific activities (1 nmol of phosphate hydrolyzed from model substrate/min) based on information provided by vendors, and all were active against synthetic substrates as described (*38*). Reactions were performed for 2 h at 22 °C followed by elution of proteins from beads with sample buffer and analysis by SDS-PAGE/autoradiography or immunoblotting. Parallel reactions were performed with immunoprecipitated metabolically phosphorylated rat striatal DAT to compare dephosphorylation patterns of NDAT and rDAT. Autoradiographs were scanned and $^{32}$P labeling intensities of untreated samples were defined as 100% with treatment values expressed as a fraction therof. Normalized phosphorylation values from multiple experiments were averaged and analyzed statistically by analysis of variance (ANOVA) using Prism 3 software.

*Asp-N Proteolysis of rDAT.* Membranes were prepared from rat striatal slices metabolically labeled with $^{32}PO_4$ and treated with OA and oleoyl acetyl glycerol (OAG) to stimulate DAT phosphorylation, followed by in situ proteolysis with endoproteinase Asp-N as described previously (*34*). Membranes were solubilized, and DAT and DAT fragments were subjected to immunoprecipitation with Ab16 followed by electrophoresis, autoradiography, and phosphoamino acid analysis.

*T53A Mutagenesis.* The T53A mutation was made in the rDAT pcDNA 3.1 template using the Stratagene quick change kit followed by sequencing of the entire DAT region to ensure accuracy. $LLCPK_1$ cells were stably transfected with the vector using FuGENE transfection reagent and maintained under selection with 600 $\mu$g/mL G418. Total and surface DAT expression and DA uptake kinetic parameters of the T53A DAT were not significantly different from the WT protein (not shown).

*Phosphoamino Acid Analysis.* NDAT, rDAT, and Asp-N fragments were subjected to phosphoamino acid analysis by two-dimensional thin layer chromatography (2D TLC) (*39*). $^{32}$P-labeled samples, prepared as described above, were electrophoresed on SDS-PAGE, detected by autoradiography and excised. Protein was electroeluted, dialyzed against distilled water, acetone precipitated, and hydrolyzed with 5.7 M HCl for 2 h at 110 °C. The resulting samples were suspended in pH 1.9 buffer (acetic acid 7.8%, formic acid 2.5%) and mixed with 10 $\mu$g unlabeled phosphoserine (pSer), phosphothreonine (pThr), and phosphotyrosine (pTyr) standards. Samples were spotted onto cellulose thin layer plates and electrophoresed using a Hunter thin layer electrophoresis unit at 1.5 kV for 35 min at pH 1.9 in the first dimension and at 1.3 kV for 20 min at pH 3.5 (pyridine 0.5%, acetic acid 5%) in the second dimension. Standards were visualized with ninhydrin, and the plates were subjected to autoradiography for 1−3 weeks.

*Materials.* IMPACT-CN bacterial cloning and expression kit, restriction enzymes, and modifying enzymes were from New England Biolabs (Ipswich, MA); [$\gamma^{32}$P]ATP (specific activity 7000 Ci/mL) and carrier-free $^{32}PO_4$ were from ICN; low- and high-range Rainbow molecular mass standards were from GE Health Care; protein kinases, protein phosphatases, OA, OAG and endoproteinase AspN were from Calbiochem (San Diego, CA); QuikChange mutagenesis kit was from Stratagene (La Jolla, CA); Complete Mini protease inhibitor tablets were from Roche Applied Bioscience (Indianapolis, IN); isopropyl $\beta$-D-1-thiogalactopyranoside (IPTG) and all other fine chemicals were from Sigma (St. Louis, MO). All

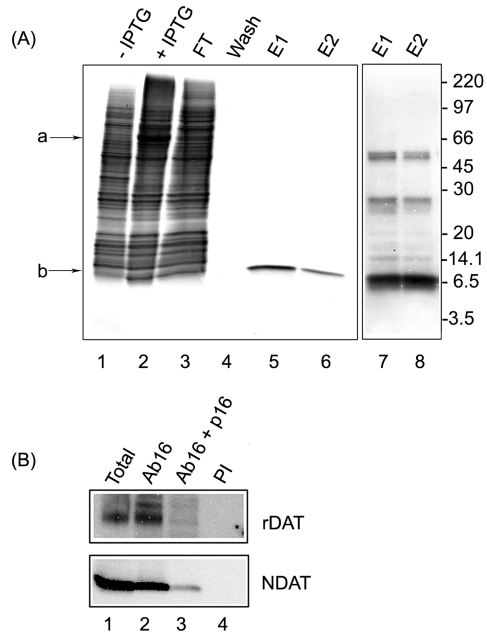


FIGURE 2: Generation and characterization of NDAT. (A) Soluble lysates were prepared from *E. coli* cells transfected with the NDAT-pTYB2 vector and treated with or without IPTG. Lysate from IPTG-induced cells was affinity purified on chitin−Sepharose and subjected to SDS-PAGE and staining with Coomassie blue (lanes 1−6) or immunoblotting with mAb16 (lanes 7 and 8): lane 1, noninduced cells; lane 2, IPTG-induced cells; lane 3 column flow through; lane 4, final wash fraction; lanes 5 and 6, sequential elution fractions; lanes 7 and 8, elution fractions immunoblotted with mAb16. (Arrow A) NDAT−CBD fusion protein. (Arrow B) NDAT. (B) rDAT (upper panel) or NDAT (lower panel) were immunoprecipitated with Ab16 and analyzed by immunoblotting with mAb16: lane 1, input samples; lanes 2 and 3, samples precipitated without (lane 2) or with (lane 3) peptide 16 preabsorption; lane 4, sample precipitated with preimmune (PI) serum. Molecular mass standards are shown in kDa.

kinases used were expressed recombinantly and were human isoforms except for CaMKII and PKGIα, which were rat and bovine isoforms, respectively. ERK1, ERK2, and Akt were phosphorylation activated. PP1α and PP2B were recombinant rabbit and human isoforms, respectively. PP2A was from bovine kidney. All enzymes were highly purified (>90−95%) as indicated by vendor's information.

## RESULTS

*Generation of Recombinant NDAT.* IPTG induction of *E. coli* cells transformed with the NDAT-pTBY2 vector (Figure 2A) caused robust production of NDAT−CBD fusion protein, which was visible at ∼65 kDa in lane 2 (arrow a) but not seen in noninduced cells (lane 1). The fusion protein was isolated from crude lysates by chromatography on chitin−Sepharose resin. NDAT−CBD bound to the resin and was not present at significant levels in the column flow-through (lane 3) or final wash fraction (lane 4). NDAT was released from CBD by incubation of resin with DTT and was visible as the major band at the expected mass of ∼7 kDa (lanes 5 and 6). The fragment was strongly reactive with N-terminal Ab16 in immunoblotting (lanes 7 and 8) and immunoprecipitation assays (Figure 2B, lower panel). Minor amounts of higher $M_r$ NDAT aggregates were also visible in Coomassie stained and immunoblotted samples. Similar to the pattern obtained with rDAT (Figure 2B, upper panel),

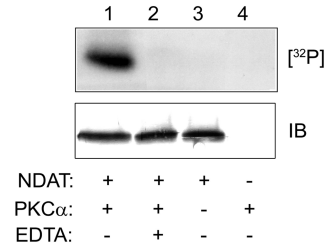


FIGURE 3: In vitro phosphorylation of NDAT. NDAT was incubated with PKCα in a reaction mixture containing [$\gamma$-$^{32}$P]ATP and the indicated components. Lane 1, control reaction mixture; lane 2, reaction contained 100 mM EDTA; lane 3, reaction contained no PKCα; lane 4, reaction contained no NDAT. Samples were immunoprecipitated with Ab16 and analyzed by SDS-PAGE/autoradiography (upper panel) or immunoblotting (IB) (lower panel).

NDAT precipitation with Ab16 (Figure 2B, lane 2) was blocked by antibody preabsorption with immunizing peptide (lane 3) and was not obtained with preimmune antiserum (lane 4), verifying the identity of the recombinant peptide. These procedures produce a final yield of 2−5 mg of NDAT per liter of *E. coli* culture with an estimated purity of ≥95%.

*Multiple Kinases Phosphorylate NDAT in Vitro.* We then tested the ability of NDAT to serve as an in vitro substrate for various purified serine/threonine kinases. Because of the substantial evidence demonstrating PMA stimulation of DAT metabolic phosphorylation, our initial studies focused on PKC (Figure 3). Lane 1 (upper panel) shows an autoradiograph of NDAT $^{32}$P labeling catalyzed by PKCα. Labeling was blocked by chelation of $Mg^{2+}$ with EDTA to prevent phosphoryl transfer (lane 2), and reactions in which either NDAT or PKCα was absent showed no $^{32}$P-labeled product (lanes 3 and 4). Western blotting demonstrated the presence of NDAT in all pertinent reactions (lower panel). These controls substantiate the identities of the phosphorylated product as NDAT and the kinase as PKCα and validate the assay as demonstrating NDAT in vitro phosphorylation.

We then extended these studies to other kinases (Figure 4), using equal enzyme activities for each reaction. Figure 4A,C shows representative results from separate experiments in which the kinases indicated in each panel were tested in parallel. Upper rows of each panel show autoradiographs of $^{32}$P incorporation, and lower rows show immunoblots verifying equal NDAT loading. The results show that NDAT was capable of serving as an in vitro substrate for PKCα, PKCβI, PKCβII, PKCγ, ERK1, ERK2, CaMKII, PKA catalytic subunit, cGMP dependent protein kinase (PKG), casein kinase II (CKII), p38, c-Jun-N-terminal kinase (JNK), cyclin dependent kinase 5 (Cdk5), and Akt. Of the kinases we tested, only GSK3β failed to catalyze detectable NDAT phosphorylation. Marked differences in $^{32}$P labeling were observed (Figure 4B,D), with comparable levels obtained with PKCα, PKA, CaMKII, and CKII; considerably higher levels catalyzed by ERK1/2, JNK, p38, PKG, and Cdk5; and lower levels catalyzed by PKCβI, PKCβII, PKCγ, and Akt.

The highest level of NDAT phosphorylation in these experiments was consistently obtained with the proline-directed kinases ERK1/2, p38, and JNK, which catalyzed 5−8 times more $^{32}$P incorporation than PKCα (Figure 4B). Immunoblots of NDAT phosphorylated by ERK1/2, p38 and JNK showed a discrete upward electrophoretic mobility shift compared with that of NDAT that was unphosphorylated or

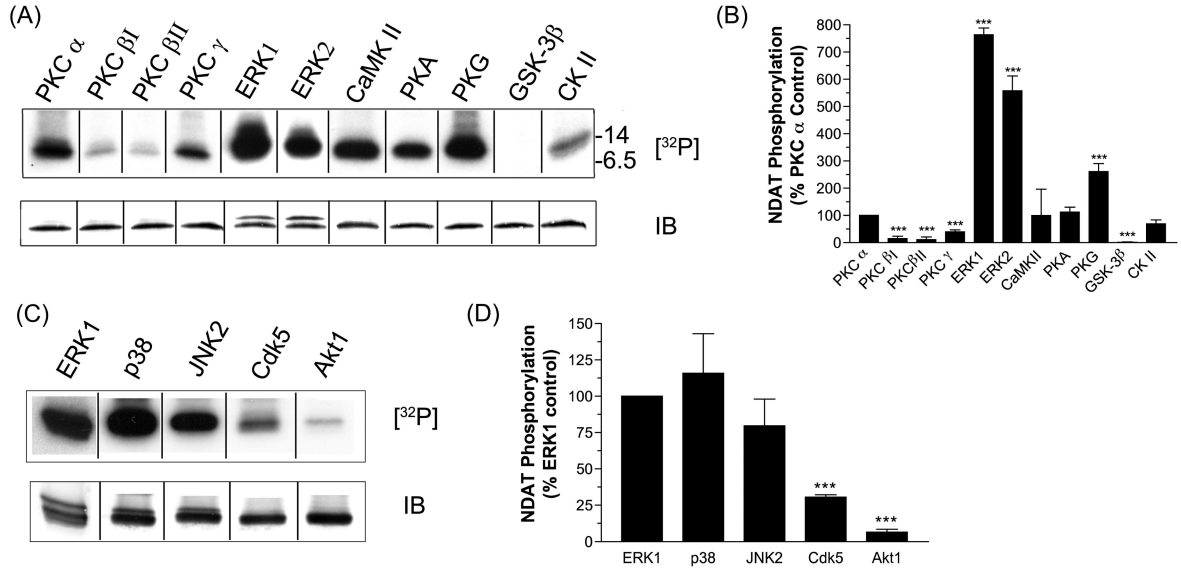


FIGURE 4: Multiple kinases phosphorylate NDAT. Equal amounts of NDAT were subjected to in vitro phosphorylation with the indicated protein kinases followed by immunoprecipitation with Ab16 and SDS-PAGE/autoradiography (upper panels) or immunoblotting (IB) (lower panels). Panels A and C represent separate experiments with the immunoblot and autoradiograph obtained from aliquots of the same samples electrophoresed on separate gels in panel A, and the autoradiograph obtained from the immunoblot in panel C. Panels B and D show quantification of phosphorylation levels (means ± SE of two independent experiments) relative to PKCα (B) or ERK1 (D). (∗∗∗)$p < 0.001$ relative to indicated control.

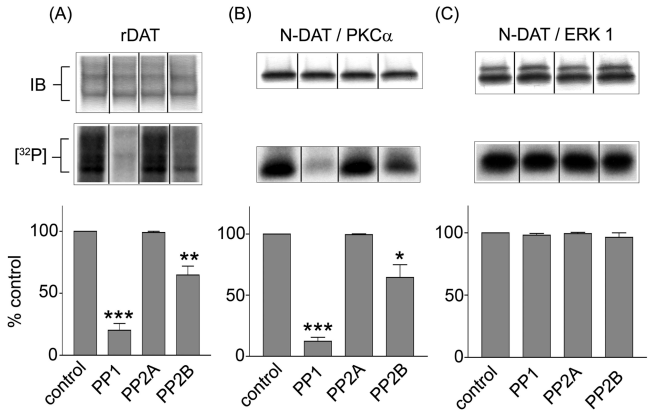


FIGURE 5: In vitro dephosphorylation of NDAT. Metabolically phosphorylated rat striatal DAT (A) or NDAT phosphorylated in vitro by PKCα (B) or NDAT phosphorylated in vitro by ERK1 (C) were immunoprecipitated and immune complexes incubated with PP1, PP2A or PP2B followed by immunoblotting (upper panel) or SDS-PAGE/autoradiography (middle panel). Gel lanes correspond to treatments indicated directly below on histogram. Lower panel: quantification of NDAT or rDAT phosphorylation levels relative to control (means ± SE of three independent experiments). (∗) $p < 0.05$ relative to control; (∗∗) $p < 0.01$ relative to control; (∗∗∗) $p < 0.001$ relative to control, by ANOVA.

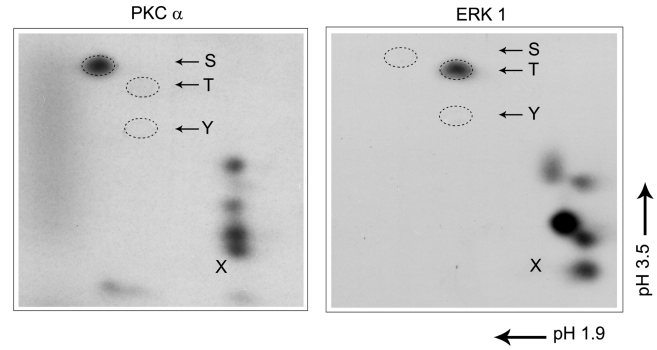


FIGURE 6: Phosphoamino acid analysis of NDAT. NDATs phosphorylated by PKCα or ERK1 were gel purified and subjected to acid hydrolysis and 2D TLC in the presence of phosphoamino acid standards (dotted circles) followed by autoradiography. X, sample origin; S, pSer; T, pThr; and Y, pTyr.

phosphorylated by other kinases (Figures 4, 5 and 7), with the fraction of NDAT present in the upper band ranging from 25−75% of the total sample. Alignment of autoradiographs with immunoblots of radiolabeled samples showed that all of the $^{32}$P was associated with the upper band, suggesting that phosphorylation of NDAT by these kinases induced a conformational change that resulted in reduced electrophoretic mobility. Confirmation that the shift was induced by phosphorylation was obtained in studies described below.

Further characterization of NDAT phosphorylation by PKCα and ERK1 showed that at the NDAT concentrations used in these experiments, $^{32}$P labeling was linear up to 2 h of incubation, with no significant increases in labeling observed with higher doses of enzyme (not shown), which indicated that under these conditions NDAT phosphorylation progressed to near completion. At the concentrations of PKCα and ERK1 used in these studies, NDAT saturation analyses generated $K_m$ values of 2.5 and 4 $\mu$M, respectively (not shown). These values are comparable to or lower than the $K_m$ values of many kinases for peptide substrates (*39, 40*), indicating that NDAT is an excellent substrate for these enzymes. Because the NDAT electrophoretic mobility shift induced by ERK1 is caused by phosphorylation, the fraction of shift (25−75%) provides an estimated phosphorylation stoichiometry of 0.25−0.75 mol phosphate/mol protein for ERK1. A comparable stoichiometry estimate of ∼0.2 mol phosphate/mol protein was obtained by scintillation counting of $^{32}$P-labeled NDAT. Comparison of samples phosphorylated in parallel by PKCα, CaMKII, PKA, and PKG then generates estimates of approximately 0.05−0.15 mol phosphate/mol protein for these enzymes. The significantly lower levels of NDAT phosphorylation catalyzed by PKC$\beta$I, PKC$\beta$II, PKC$\gamma$, and Akt are consistent with low affinity/low stoichiometry interactions that may be less likely to occur

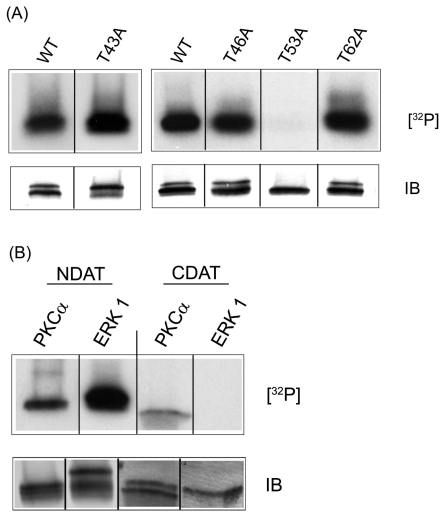


FIGURE 7: ERK1 phosphorylates NDAT on Thr53. (A) Equal amounts of WT or T → A mutant NDATs were incubated with ERK1 under phosphorylation conditions followed by immunoprecipitation and autoradiography (upper panel) or immunoblotting (lower panel). Samples in left and right panels were analyzed in separate experiments. (B) Equal amounts (1.5 $\mu$g) of NDAT or CDAT were subjected to phosphorylation conditions with PKCα or ERK1 followed by immunoprecipitation and SDS-PAGE/autoradiography (upper panel) or immunoblotting (lower panel).

physiologically, and further studies with these enzymes were not performed.

*In Vitro Dephosphorylation of NDAT.* We then used NDAT phosphorylated by PKCα or ERK1 as a substrate for analysis of in vitro dephosphorylation by purified PP1, PP2A or PP2B, and monitored dephosphorylation of rDAT in parallel (Figure 5). The phosphatases were used at equal specific activities, and all were active against model substrates as previously described (*38*). Phosphorylation levels were monitored by SDS-PAGE/autoradiography (middle row) and Western blotting confirmed the presence of equal amounts of NDAT or rDAT in all samples (upper row). Quantification of $^{32}$P labeling relative to control samples is shown in histograms (lower row). For NDAT phosphorylated by PKCα, the greatest level of dephosphorylation was catalyzed by PP1, which removed 88 ± 3% of the $^{32}$P label, a lesser amount was catalyzed by PP2B, which removed 35 ± 10% of the $^{32}$P label, and no dephosphorylation was obtained with PP2A (Figure 5B). A similar profile was obtained for rDAT metabolically phosphorylated under PKC stimulation conditions (Figure 5A) suggesting the similarity of phosphatase action on NDAT and full-length DAT. In contrast to these results, treatment of ERK1-phosphorylated NDAT with these phosphatases caused no removal of $^{32}$P or alteration in electrophoretic mobility shift (Figure 5C).

*Phosphoamino Acid Analysis of NDAT.* The N-terminal tail of DAT contains eight serines and four threonines (Figure 1A). To determine the type of amino acid phosphorylated in NDAT, we subjected PKCα and ERK1 phosphorylated NDAT to phosphoamino acid analysis (Figure 6). The results show that phosphorylation of NDAT by PKCα occurred to detectable levels only on Ser while phosphorylation catalyzed by ERK1 occurred only on Thr, demonstrating the use of distinct sites by these kinases. Phosphorylation of NDAT by PKA, PKG and CaMKII also occurs exclusively on Ser (*40*).

*Identification of ERK Phosphorylation Site.* In an attempt to identify the sites of PKCα phosphorylation on NDAT, we constructed individual S → A substitutions of the first five serines and found that phosphorylation was reduced but not eliminated in some of the mutants, indicating that PKCα phosphorylates NDAT at multiple sites (*40*). This parallels mutagenesis findings consistent with occurrence of PMA-stimulated rDAT metabolic phosphorylation on multiple serines (*35*), and we are currently attempting to ascertain the precise pattern of NDAT phosphorylation by PKCα.

To investigate ERK phosphorylation sites, we generated individual T → A substitutions of NDAT at positions 43, 46, 53, and 62 and subjected the mutants to in vitro phosphorylation with ERK1 (Figure 7A). The T43A, T46A, and T62A NDATs displayed $^{32}$P labeling that was not less than the WT levels (upper panel) and showed the upward electrophoretic mobility shift (lower panels), while T53A NDAT showed no $^{32}$P labeling or upward shift. T53A NDAT treated with p38 or JNK also showed no $^{32}$P incorporation or mobility shift (not shown). These results indicate that Thr53 is the sole phosphorylation site for ERK1, p38, and JNK, and verify that the mobility shift is caused by phosphorylation.

In rDAT, Thr53 is located in a sequence (P-P-Q-T-P) that conforms to an optimal proline-directed kinase consensus motif (P-P-X-S/T-P, where P is proline and X is any amino acid) (*41*) that is consistent with its use in vitro. An analogous proline-directed phosphorylation motif (P-R-Q-S-P) is present in hDAT (Figure 1A), indicating the conservation of the sequence. The C-terminal tail of rDAT contains a minimal proline-directed phosphorylation sequence (S/T-P) at residues Thr595-Pro596, a site that is not conserved in hDAT (Figure 1B). To determine if the C-terminal site of rDAT also undergoes phosphorylation, we expressed and purified the CDAT recombinant protein extending from residues 579−619 (approximate mass 4 kDa) in a manner analogous to that of NDAT and subjected the peptide to in vitro phosphorylation. Figure 7B shows that ERK1 does not phosphorylate CDAT under the conditions positive for NDAT, indicating the specificity of NDAT phosphorylation by ERK. CDAT is also a negligible substrate for PKCα, with a phosphorylation level of <10% of that of PKCα-phosphorylated NDAT.

*In Vivo Threonine Phosphorylation of DAT Occurs on the N-terminal Tail.* To probe the potential similarities between NDAT and rDAT threonine phosphorylation, we directed our efforts to determining the site of metabolic threonine phosphorylation on rDAT. Phosphoamino acid analysis of $^{32}$P-labeled rat striatal DAT has shown the presence of pSer and pThr at about a 10:1 ratio (*34*). However, the origin of pThr in DAT is unknown, as the major site of metabolic phosphorylation at the distal end of the N-terminus contains no Thr residues (Figure 1A), and there are numerous Thr in the N- and C-termini and intracellular loops that could function as phosphorylation sites.

To determine the origin of pThr on native DAT, we used peptide mapping with endoproteinase Asp-N in combination with phosphoamino acid analysis. Asp-N cleaves DAT at Asp175 at the extracellular end of transmembrane domain (TM) 3, generating a 19 kDa fragment that extends from the N-terminus through TMs 1−3 (*34*). This fragment contains only six threonines (Thr43, Thr46, Thr53, Thr62, Thr144, and Thr172), and molecular modeling strongly

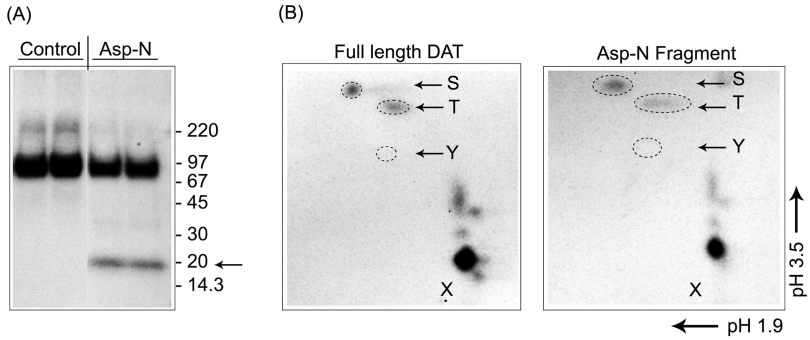


FIGURE 8: Identification of phosphothreonine in the rDAT N-terminal tail. (A) Membranes from $^{32}P$ metabolically labeled rat striatal slices were treated with endoproteinase Asp-N followed by immunoprecipitation with Ab16 and SDS-PAGE/autoradiography. Full-length DAT and Asp-N fragments (arrow) were excised from the gel and processed for phosphoamino acid analysis. (B) TLC plates containing samples from the full-length DAT and Asp-N fragments were subjected to autoradiography, and phosphoamino acid standards were visualized with ninhydrin (dotted circles). Key: X, origin; S, pSer; T, pThr; and Y, pTyr.

suggests that only the four in the N-terminal tail are intracellularly oriented and thus capable of serving as phosphate acceptors, while the other two are embedded in the membrane or oriented extracellularly (*42*). This strategy thus provides a method for analyzing phosphorylation of N-terminal Thr residues independently of sites elsewhere in the protein.

For this experiment, we metabolically labeled rat striatal slices with $^{32}P$ in the presence of OA and OAG to stimulate DAT phosphorylation and subjected membranes prepared from the slices to in situ proteolysis with Asp-N. The samples were precipitated with Ab16 to isolate the $^{32}P$-labeled full-length DATs and the N-terminal Asp-N fragment (Figure 8A), and the bands were excised from the gel and subjected to phosphoamino acid analysis. Equal counts were loaded to permit comparison of pSer and pThr ratios, and samples precipitated with preimmune antiserum were processed in parallel to test for signal specificity.

Figure 8B shows that both pSer and pThr are present in the full-length DAT and the Asp-N fragment. No radioactive pSer or pThr were obtained from samples precipitated with preimmune serum (not shown), verifying that the extracted phosphoamino acids originated from DAT. Because the only intracellular threonines in the Asp-N fragment are the four in the N-terminal tail, this result identifies one or more of these residues as a source of pThr in neuronal DAT. In addition, because all known serine phosphorylation on DAT originates from the N-terminal tail, the similar ratios of pSer and pThr in full-length DAT and the Asp-N fragment indicate that a significant fraction of the pThr in the intact protein originates from the N-terminus.

To determine if Thr53 represents the site of phosphothreonine incorporation on DAT, we expressed the T53A rDAT mutant and performed phosphoamino acid analysis of $^{32}P$ metabolically labeled protein. In preliminary experiments, we found that T53A rDAT displayed basal and PMA-stimulated phosphorylation that was not qualitatively different from the WT phosphorylation pattern (not shown). Figure 9A shows the phosphorylation profile of the WT and T53A proteins and a sample from DAT-null cells that was labeled and processed in parallel to serve as a specificity control. The DAT regions of these gels were excised, and the extracted proteins processed for phosphoamino acid analysis. Both pSer and pThr were obtained from the WT protein (Figure 9B, left), while no detectable radioactivity was

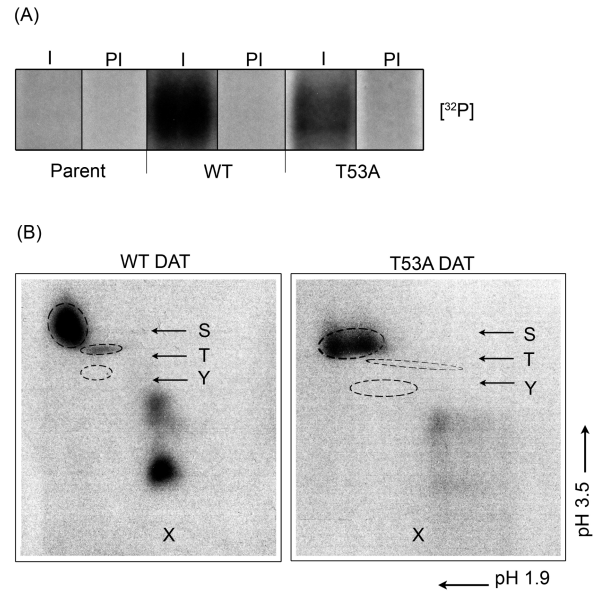


FIGURE 9: Phosphothreonine is not present in T53A rDAT. $LLCPK_1$ cells expressing WT or T53A rDAT were labeled with $^{32}PO_4$ and treated with 1 $\mu$M PMA for 30 min. Samples from parent $LLCPK_1$ cells were treated and processed exactly in parallel for analysis of signal specificity. (A) Lysates were precipitated with immune (I) or preimmune (PI) serum and analyzed by SDS-PAGE/autoradiography. (B) WT and T53A DATs were extracted and equal counts subjected to phosphoamino acid analysis. Phosphoamino acid standards were visualized with ninhydrin (dotted circles). Key: X, origin; S, pSer; T, pThr; and Y, pTyr.

obtained from the parent cells (not shown), verifying that the observed pSer and pThr signals originated from DAT. The T53A protein yielded pSer as expected, as the N-terminal serine cluster was unaffected by the mutation but importantly showed no pThr signal (Figure 9B, right), strongly suggesting that Thr53 represents a major site of metabolic pThr incorporation on DAT. This result has been replicated in an independently executed experiment.

Several studies have shown that ERK inhibitors reduce DA uptake (*14, 16*). To determine if phosphorylation of DAT at Thr53 is involved in this response, we treated cells expressing WT and T53A rDAT with the ERK inhibitor PD98059 and assayed for DA transport activity. Compared to transport activity in control treatments, transport activity after treatment of cells with 50 $\mu$M PD98059 for 30 min was reduced to 63 $\pm$ 2% in the WT cells and to 70 $\pm$ 3% in the T53A cells, indicating that down-regulation to this

treatment is not dependent on the phosphorylation state of Thr53. Acute down-regulation of transport to 1 $\mu$M PMA was also not affected by the mutation (not shown).

## DISCUSSION

In this study, we found that NDAT was an excellent substrate for in vitro phosphorylation by PKCα, CaMKII, PKA, PKG, ERK1/2, p38, and JNK, and for in vitro dephosphorylation by PP1 and PP2B, demonstrating the capability of these enzymes to directly act on the DAT N-terminal domain. Many of the in vitro phosphorylation characteristics we found were highly similar to what had been previously known for in vivo phosphorylation, including the presence of pSer and pThr on NDAT and the rDAT N-terminal tail, localization of PKC-mediated phosphorylation to multiple sites in the distal N-terminal serine cluster, the most robust dephosphorylation catalyzed by PP1, and negligible phosphorylation occurring on CDAT or rDAT C-terminus. These characteristics in conjunction with the good stoichiometry and kinetic values of the in vitro reactions support the potential for these enzymes to act on DAT in vivo. The in vitro findings also led us to examine additional conditions related to PKA, PKG, and proline-directed kinases that have now considerably expanded our understanding of DAT phosphorylation characteristics.

The kinases we tested that strongly phosphorylated NDAT on Ser were PKCα, PKA, PKG, and CaMKII. DAT metabolic phosphorylation has been well characterized to be stimulated by PMA, activation of PKC-linked receptors, and METH and AMPH via a PKC-dependent pathway (*13, 18, 30, 34*). In all of these cases, the site of phosphorylation has been localized to the distal N-terminal serine cluster; thus the phosphorylation of NDAT on Ser by PKCα strongly supports the potential for the in vivo phosphorylation stimulated under these conditions to be catalyzed directly by PKCα. With respect to other kinases, we have recently found that DAT phosphorylation is increased by activators of PKA and PKG (A. Moritz and R. Vaughan, unpublished results), which could potentially be consistent with the NDAT results; although in these cases, we have not yet identified the phosphorylation sites. For PKG a site outside the N-terminus may be a possibility, as the closely related serotonin transporter undergoes PKG-dependent phosphorylation at a canonical PKG site in IL2 that is conserved in DAT (*43*). Finally, CaMKII has been invoked to phosphorylate DAT based on loss of CaMKII-dependence of AMPH-induced DA efflux after mutagenesis of N-terminal serines (*15*). Although regulation of DAT phosphorylation in response to modulation of CaMK has not been demonstrated, the robust phosphorylation of NDAT and DAT N-terminal peptide by CaMKII (*15*) supports this possibility.

Of the kinases we characterized for phosphoamino acid usage, the only ones that phosphorylated NDAT on Thr were the proline-directed kinases ERK1/2, p38, and JNK. These kinases require a proline immediately following the phosphoacceptor site, and catalyzed robust phosphorylation of Thr53 present within a proline-directed kinase motif close to the intracellular end of TM1. We verified the presence of pThr on the N-terminal tail of neuronal DAT and identified Thr53 as a phosphorylation site in heterologously expressed DAT. Because proline-directed motifs are not recognized by nonproline directed kinases, these findings demonstrate that DAT is a direct in vivo substrate for ERK or other proline-directed kinases. We have not yet attempted to modulate phosphorylation of this site by activators or inhibitors of any of these kinases, so the identities of the enzymes that regulate this site remain to be determined. However, the potential for ERK to catalyze the Thr phosphorylation of DAT in vivo is supported by the suppression of DAT phosphorylation by the MEK inhibitor U0126 (*32*).

Several of the kinases that we tested (PKC$\beta$I, PKC$\beta$II, PKC$\gamma$, and Akt) showed considerably lower activity against NDAT compared with the case for ERK1 or PKCα. This suggests a lower probability for these kinases to act on DAT, although we cannot exclude the possibility that in vivo interactions with these kinases could be promoted by adaptor proteins or other conditions not present in vitro. As some of these kinases (PKC$\beta$II and Akt) participate in DAT regulatory mechanisms (*14, 21*), our findings are more consistent with effects of these pathways being mediated indirectly rather than through direct phosphorylation of DAT. The only kinase we tested that showed no detectable reaction with NDAT was GSK3$\beta$. However, GSK3$\beta$ often requires a priming phosphorylation event on its substrates by a distinct kinase at a separate phosphoacceptor site (*44*); thus we do not know if our result for NDAT represents a true negative for GSK3$\beta$ phosphorylation or a manifestation of a requirement for priming.

Of the kinases we tested, the highest stoichiometry of NDAT phosphorylation was catalyzed by ERK1/2, p38, and JNK, which also induced a conformational change that altered the peptide electrophoretic mobility. This confomational change is likely to be caused by cis-isomerization of the pThr-Pro bond, which is characteristic of proline-directed phosphorylation and well established to induce significant alterations in protein secondary structure (*45*). Whether phosphorylation at this site in vivo could be related to the multiple DAT bands commonly seen in Western blots (*37, 46*) or to previously noted upward shifts of DAT that accompany metabolic phosphorylation (*13*) is not known. However, the induction of such a conformational change by phosphorylation of Thr53 could significantly impact the properties of this domain.

Our finding that Thr53 is phosphorylated in vivo provides the first localization of pThr on DAT, and the first evidence that phosphorylation occurs in the membrane proximal region of the N-terminal tail. Phosphorylation of this residue is not required for down-regulation mediated by ERK inhibition or PMA, and future work will be required to determine the function of this site. At present, little is known about the structures or functions of the DAT cytosolic domains or how they might be affected by phosphorylation. Our current understanding of DAT structure is based on homology to the bacterial leucine transporter (LeuT), which does not possess the extensive cytoplasmic domains found in DAT (*47*), and provides little guidance regarding this issue. However, the proximity of phosphorylation to the intracellular end of TM1 suggests the potential to impact functions associated with this domain, including binding and permeation of substrates, binding of cocaine and other transport blockers, and ionic interactions between Arg60 and other intracellular gate residues (*42, 48*−*50*). Proline-rich regions, such as that surrounding Thr53, can also serve as binding

sites for Src homology 3 domain proteins (*51*), which function to regulate protein−protein interactions. One possibility for function is interaction with DAT binding partners such as syntaxin (*52*), which could affect ion flow or efflux. The structural changes induced by PKC-dependent phosphorylation of the distal serine cluster, and how these impact DAT functions, are also unknown.

Very little is known about the role of dephosphorylation in DAT regulation. We previously found in rat striatal tissue that OA treatment down-regulates DA transport activity and leads to strong elevations in DAT phosphorylation indicative of significant tonic dephosphorylation (*13, 38*). In the present study we found that NDATs phosphorylated by PKCα were extensively dephosphorylated by PP1, which parallels our previous findings of robust PP1-induced in vivo and in vitro dephosphorylation of PKC- and OA-stimulated phosphorylation sites on rDAT (*38*) and provides further evidence supporting the role of PP1 as the major DAT phosphatase. We also found for the first time that PP2B (calcineurin) caused a partial level of NDAT and rDAT dephosphorylation. The basis for the differential levels of NDAT and rDAT dephosphorylation by PP1 and PP2B is not known, although potential reasons include enzyme affinity for the peptide, phosphorylation site accessibility, and activity against different subsets of residues. Further work will be required to determine if DAT is dephosphorylated in vivo by PP2B, but if this occurs it would indicate the potential for a previously unknown mode of regulation of DAT phosphorylation levels by $Ca^{2+}$-calmodulin dependent mechanisms. Our finding that PP2A does not detectably dephosphorylate PKCα-phosphorylated NDAT or PMA-phosphorylated rDAT is consistent with our previous in vitro results and supports the lack of major PP2A effects on metabolic phosphorylation (*38*). However, further work is necessary to examine the role of PP2A, as the in vitro PP2A studies were performed with purified catalytic subunit that lacks the scaffolding and regulatory subunits that may be necessary for driving enzyme−substrate interactions.

In contrast to our findings of significant in vitro dephosphorylation of PKC-catalyzed phosphorylation sites, none of the tested phosphatases were able to dephosphorylate ERK-phosphorylated NDATs. This may indicate that pThr53 requires a phosphatase different from those tested or that the altered conformation induced by Thr53 phosphorylation generates a peptide structure resistant to dephosphorylation. For many proteins including tau, Cdc25 and myc, ERK-catalyzed phosphorylation is removed primarily by PP2A, but this occurs only after the cis pSer/pThr-Pro conformation induced by phosphorylation is converted to the trans form by peptidyl−prolyl cis/trans isomerase (*45, 53*). This could explain the phosphatase resistance of NDAT, because the cis/trans isomerization necessary to allow PP2A to dephosphorylate the peptide could not occur in vitro. Evidence that PP2A binds to DAT (*54*) suggests a role for this enzyme in DAT function. Our findings that DAT phosphorylation is only slightly increased by PP2A specific inhibitors (*38*), in conjunction with a lack of PP2A effects on PKC-catalyzed sites could be consistent with a role for this enzyme at Thr53 or other site(s) distinct from those in the PKCα phosphorylated domain.

The results presented in this study demonstrate the ability of the recombinant DAT N-terminal domain to directly interact with several protein kinases and phosphatases and for phosphorylation to occur at distinct sites. This is consistent with the regulation of DAT in vivo phosphorylation levels by multiple kinases (PKC, PKA, PKG, and ERK) and phosphatases (PP1 and PP2A) occurring by direct action of these enzymes. Phosphorylation of DAT by multiple kinases at distinct and/or overlapping sites could serve as a mechanism for integration of information from multiple pathways, or could provide a mechanism for different pathways to regulate distinct transporter functions. Because increasing evidence indicates that DAT regulation occurs by a combination of direct transporter phosphorylation and phosphorylation of interacting proteins (*15, 18, 30, 55*), determining the details of these events is crucial for elucidating the mechanisms by which incoming physiological signals impact DA clearance in normal and disease states.

## REFERENCES


1. Giros, B., Jaber, M., Jones, S. R., Wightman, R. M., and Caron, M. G. (1996) Hyperlocomotion and indifference to cocaine and amphetamine in mice lacking the dopamine transporter. *Nature 379*, 606–612.
2. Kuhar, M. J., Ritz, M. C., and Boja, J. W. (1991) The dopamine hypothesis of the reinforcing properties of cocaine. *Trends Neurosci. 14*, 299–302.
3. Eshleman, A. J., Henningsen, R. A., Neve, K. A., and Janowsky, A. (1994) Release of dopamine via the human transporter. *Mol. Pharmacol. 45*, 312–316.
4. Sulzer, D., Chen, T. K., Lau, Y. Y., Kristensen, H., Rayport, S., and Ewing, A. (1995) Amphetamine redistributes dopamine from synaptic vesicles to the cytosol and promotes reverse transport. *J. Neurosci. 15*, 4102–4108.
5. Weinberger, D. R., Egan, M. F., Bertolino, A., Callicott, J. H., Mattay, V. S., Lipska, B. K., Berman, K. F., and Goldberg, T. E. (2001) Prefrontal neurons and the genetics of schizophrenia. *Biol. Psychiatry 50*, 825–844.
6. Tintner, R., and Jankovic, J. (2002) Treatment options for Parkinson's disease. *Curr. Opin. Neurol. 15*, 467–476.
7. Sawa, A., and Snyder, S. H. (2002) Schizophrenia: diverse approaches to a complex disease. *Science 296*, 692–695.
8. Olanow, C. W. (2002) The role of dopamine agonists in the treatment of early Parkinson's disease. *Neurology 58*, S33–S41.
9. Mazei-Robison, M. S., Bowton, E., Holy, M., Schmudermaier, M., Freissmuth, M., Sitte, H. H., Galli, A., and Blakely, R. D. (2008) Anomalous dopamine release associated with a human dopamine transporter coding variant. *J. Neurosci. 28*, 7040–7046.
10. Zahniser, N. R., and Doolen, S. (2001) Chronic and acute regulation of Na+/Cl- -dependent neurotransmitter transporters: drugs, substrates, presynaptic receptors, and signaling systems. *Pharmacol. Ther. 92*, 21–55.
11. Melikian, H. E. (2004) Neurotransmitter transporter trafficking: endocytosis, recycling, and regulation. *Pharmacol. Ther. 104*, 17–27.
12. Vaughan, R. A. (2004) Phosphorylation and regulation of psychostimulant-sensitive neurotransmitter transporters. *J. Pharmacol. Exp. Ther. 310*, 1–7.
13. Vaughan, R. A., Huff, R. A., Uhl, G. R., and Kuhar, M. J. (1997) Protein kinase C-mediated phosphorylation and functional regulation of dopamine transporters in striatal synaptosomes. *J. Biol. Chem. 272*, 15541–15546.
14. Garcia, B. G., Wei, Y., Moron, J. A., Lin, R. Z., Javitch, J. A., and Galli, A. (2005) Akt is essential for insulin modulation of amphetamine-induced human dopamine transporter cell-surface redistribution. *Mol. Pharmacol. 68*, 102–109.
15. Fog, J. U., Khoshbouei, H., Holy, M., Owens, W. A., Vaegter, C. B., Sen, N., Nikandrova, Y., Bowton, E., McMahon, D. G., Colbran, R. J., Daws, L. C., Sitte, H. H., Javitch, J. A., Galli, A., and Gether, U. (2006) Calmodulin kinase II interacts with the dopamine transporter C terminus to regulate amphetamine-induced reverse transport. *Neuron 51*, 417–429.
16. Moron, J. A., Zakharova, I., Ferrer, J. V., Merrill, G. A., Hope, B., Lafer, E. M., Lin, Z. C., Wang, J. B., Javitch, J. A., Galli, A., and Shippenberg, T. S. (2003) Mitogen-activated protein kinase regulates dopamine transporter surface expression and dopamine transport capacity. *J. Neurosci. 23*, 8480–8488.

17. Gulley, J. M., Doolen, S., and Zahniser, N. R. (2002) Brief, repeated exposure to substrates down-regulates dopamine transporter function in Xenopus oocytes in vitro and rat dorsal striatum in vivo. *J. Neurochem. 83*, 400–411.
18. Cervinski, M. A., Foster, J. D., and Vaughan, R. A. (2005) Psychoactive substrates stimulate dopamine transporter phosphorylation and down-regulation by cocaine-sensitive and protein kinase C-dependent mechanisms. *J. Biol. Chem. 280*, 40442–40449.
19. Gorentla, B. K., and Vaughan, R. A. (2005) Differential effects of dopamine and psychoactive drugs on dopamine transporter phosphorylation and regulation. *Neuropharmacology 49*, 759–768.
20. Kahlig, K. M., Javitch, J. A., and Galli, A. (2004) Amphetamine regulation of dopamine transport. Combined measurements of transporter currents and transporter imaging support the endocytosis of an active carrier. *J. Biol. Chem. 279*, 8966–8975.
21. Johnson, L. A., Guptaroy, B., Lund, D., Shamban, S., and Gnegy, M. E. (2005) Regulation of amphetamine-stimulated dopamine efflux by protein kinase C beta. *J. Biol. Chem. 280*, 10914–10919.
22. Saunders, C., Ferrer, J. V., Shi, L., Chen, J., Merrill, G., Lamb, M. E., Leeb-Lundberg, L. M., Carvelli, L., Javitch, J. A., and Galli, A. (2000) Amphetamine-induced loss of human dopamine transporter activity: an internalization-dependent and cocaine-sensitive mechanism. *Proc. Natl. Acad. Sci. U.S.A. 97*, 6850–6855.
23. Loder, M. K., and Melikian, H. E. (2003) The dopamine transporter constitutively internalizes and recycles in a protein kinase C-regulated manner in stably transfected PC12 cell lines. *J. Biol. Chem. 278*, 22168–22174.
24. Melikian, H. E., and Buckley, K. M. (1999) Membrane trafficking regulates the activity of the human dopamine transporter. *J. Neurosci. 19*, 7699–7710.
25. Foster, J. D., Adkins, S. D., Lever, J. R., and Vaughan, R. A. (2008) Phorbol ester induced trafficking-independent regulation and enhanced phosphorylation of the dopamine transporter associated with membrane rafts and cholesterol. *J. Neurochem. 105*, 1683–1699.
26. Johnson, L. A., Furman, C. A., Zhang, M., Guptaroy, B., and Gnegy, M. E. (2005) Rapid delivery of the dopamine transporter to the plasmalemmal membrane upon amphetamine stimulation. *Neuropharmacology 49*, 750–758.
27. Miranda, M., Wu, C. C., Sorkina, T., Korstjens, D. R., and Sorkin, A. (2005) Enhanced ubiquitylation and accelerated degradation of the dopamine transporter mediated by protein kinase C. *J. Biol. Chem. 280*, 35617–35624.
28. Daniels, G. M., and Amara, S. G. (1999) Regulated trafficking of the human dopamine transporter. Clathrin- mediated internalization and lysosomal degradation in response to phorbol esters. *J. Biol. Chem. 274*, 35794–35801.
29. Goodwin, J. S., Larson, G. A., Swant, J., Sen, N., Javitch, J. A., Zahniser, N. R., De Felice, L. J., and Khoshbouei, H. (2008) Amphetamine and methamphetamine differentially affect dopamine transporters in vitro and in vivo, *J. Biol. Chem.* in press.
30. Granas, C., Ferrer, J., Loland, C. J., Javitch, J. A., and Gether, U. (2003) N-terminal truncation of the dopamine transporter abolishes phorbol ester- and substance P receptor-stimulated phosphorylation without impairing transporter internalization. *J. Biol. Chem. 278*, 4990–5000.
31. Huff, R. A., Vaughan, R. A., Kuhar, M. J., and Uhl, G. R. (1997) Phorbol esters increase dopamine transporter phosphorylation and decrease transport Vmax. *J. Neurochem. 68*, 225–232.
32. Lin, Z., Zhang, P. W., Zhu, X., Melgari, J. M., Huff, R., Spieldoch, R. L., and Uhl, G. R. (2003) Phosphatidylinositol 3-kinase, protein kinase C, and MEK1/2 kinase regulation of dopamine transporters (DAT) require N-terminal DAT phosphoacceptor sites. *J. Biol. Chem. 278*, 20162–20170.
33. Gnegy, M. E. (2000) Ca2+/calmodulin signaling in NMDA-induced synaptic plasticity. *Crit. Rev. Neurobiol. 14*, 91–129.
34. Foster, J. D., Pananusorn, B., and Vaughan, R. A. (2002) Dopamine transporters are phosphorylated on N-terminal serines in rat striatum. *J. Biol. Chem. 277*, 25178–25186.
35. Foster, J. D., Blakely, R. D., and Vaughan, R. A. (2003) Mutational analysis of potential phosphorylation sites in the N-terminal tail of the rat dopamine transporter. Abstract Viewer/Itinerary Planner. Society for Neuroscience: Washington, DC, Program No. 167.12.
36. Chang, M. Y., Lee, S. H., Kim, J. H., Lee, K. H., Kim, Y. S., Son, H., and Lee, Y. S. (2001) Protein kinase C-mediated functional regulation of dopamine transporter is not achieved by direct phosphorylation of the dopamine transporter protein. *J. Neurochem. 77*, 754–761.
37. Vaughan, R. A., Gaffaney, J. D., Lever, J. R., Reith, M. E., and Dutta, A. K. (2001) Dual incorporation of photoaffinity ligands on dopamine transporters implicates proximity of labeled domains. *Mol. Pharmacol. 59*, 1157–1164.
38. Foster, J. D., Pananusorn, B., Cervinski, M. A., Holden, H. E., and Vaughan, R. A. (2003) Dopamine transporters are dephosphorylated in striatal homogenates and in vitro by protein phosphatase 1. *Brain Res. Mol. Brain Res. 110*, 100–108.
39. Boyle, W. J., van der Geer, P., and Hunter, T. (1991) Phosphopeptide mapping and phosphoamino acid analysis by two- dimensional separation on thin-layer cellulose plates. *Methods Enzymol. 201*, 110–149.
40. Moritz, A. E., Gorentla, B. K., and Vaughan, R. A. (2007) The N-terminal tail of the dopamine transporter is phosphorylated at multiple sites in vitro. Abstract Viewer/Itinerary Planner. Society for Neuroscience: Washington, DC, Program No. 249.21.
41. Clark-Lewis, I., Sanghera, J. S., and Pelech, S. L. (1991) Definition of a consensus sequence for peptide substrate recognition by p44mpk, the meiosis-activated myelin basic protein kinase. *J. Biol. Chem. 266*, 15180–15184.
42. Beuming, T., Shi, L., Javitch, J. A., and Weinstein, H. (2006) A comprehensive structure-based alignment of prokaryotic and eukaryotic neurotransmitter/Na+ symporters (NSS) aids in the use of the LeuT structure to probe NSS structure and function. *Mol. Pharmacol. 70*, 1630–1642.
43. Ramamoorthy, S., Samuvel, D. J., Buck, E. R., Rudnick, G., and Jayanthi, L. D. (2007) Phosphorylation of threonine residue 276 is required for acute regulation of serotonin transporter by cyclic GMP. *J. Biol. Chem. 282*, 11639–11647.
44. Frame, S., and Cohen, P. (2001) GSK3 takes centre stage more than 20 years after its discovery. *Biochem. J. 359*, 1–16.
45. Zhou, X. Z., Kops, O., Werner, A., Lu, P. J., Shen, M., Stoller, G., Kullertz, G., Stark, M., Fischer, G., and Lu, K. P. (2000) Pin1-dependent prolyl isomerization regulates dephosphorylation of Cdc25C and tau proteins. *Mol. Cell 6*, 873–883.
46. Li, L. B., Chen, N., Ramamoorthy, S., Chi, L., Cui, X. N., Wang, L. C., and Reith, M. E. (2004) The role of N-glycosylation in function and surface trafficking of the human dopamine transporter. *J. Biol. Chem. 279*, 21012–21020.
47. Yamashita, A., Singh, S. K., Kawate, T., Jin, Y., and Gouaux, E. (2005) Crystal structure of a bacterial homologue of Na+/Cl--dependent neurotransmitter transporters. *Nature 437*, 215–223.
48. Kniazeff, J., Shi, L., Loland, C. J., Javitch, J. A., Weinstein, H., and Gether, U. (2008) An intracellular interaction network regulates conformational transitions in the dopamine transporter. *J. Biol. Chem. 283*, 17691–17701.
49. Beuming, T., Kniazeff, J., Bergmann, M. L., Shi, L., Gracia, L., Raniszewska, K., Newman, A. H., Javitch, J. A., Weinstein, H., Gether, U., and Loland, C. J. (2008) The binding sites for cocaine and dopamine in the dopamine transporter overlap. *Nat. Neurosci. 11*, 780–789.
50. Indarte, M., Madura, J. D., and Surratt, C. K. (2007) Dopamine transporter comparative molecular modeling and binding site prediction using the LeuT(Aa) leucine transporter as a template. *Proteins 70*, 1033–1046.
51. Sparks, A. B., Rider, J. E., Hoffman, N. G., Fowlkes, D. M., Quillam, L. A., and Kay, B. K. (1996) Distinct ligand preferences of Src homology 3 domains from Src, Yes, Abl, Cortactin, p53bp2, PLCgamma, Crk, and Grb2. *Proc. Natl. Acad. Sci. U.S.A. 93*, 1540–1544.
52. Carvelli, L., Blakely, R. D., and DeFelice, L. J. (2008) Dopamine transporter/syntaxin 1A interactions regulate transporter channel activity and dopaminergic synaptic transmission. *Proc. Natl. Acad. Sci. U.S.A. 105*, 14192–14197.
53. Pastorino, L., Sun, A., Lu, P. J., Zhou, X. Z., Balastik, M., Finn, G., Wulf, G., Lim, J., Li, S. H., Li, X., Xia, W., Nicholson, L. K., and Lu, K. P. (2006) The prolyl isomerase Pin1 regulates amyloid precursor protein processing and amyloid-beta production. *Nature 440*, 528–534.
54. Bauman, A. L., Apparsundaram, S., Ramamoorthy, S., Wadzinski, B. E., Vaughan, R. A., and Blakely, R. D. (2000) Cocaine and antidepressant-sensitive biogenic amine transporters exist in regulated complexes with protein phosphatase 2A. *J. Neurosci. 20*, 7571–7578.
55. Mortensen, O. V., Larsen, M. B., Prasad, B. M., and Amara, S. G. (2008) Genetic Complementation Screen Identifies a Mitogen-activated Protein Kinase Phosphatase, MKP3, as a Regulator of Dopamine Transporter Trafficking. *Mol. Biol. Cell 19*, 2818–2829.

BI801696N